

SimNet: Accurate and High-Performance Computer Architecture Simulation using Machine Learning

Lingda Li, Santosh Pandey[†], Thomas Flynn, Hang Liu[†], Noel Wheeler[§], Adolfo Hoisie
Brookhaven National Laboratory, [†]Stevens Institute of Technology, [§]Laboratory for Physical Sciences
{lli, tflynn, ahoisie}@bnl.gov, [†]{spande1, hliu77}@stevens.edu, [§]nwheeler@lps.umd.edu

Abstract

While discrete-event simulators are essential tools for architecture research, design, and development, their practicality is limited by an extremely long time-to-solution for realistic applications under investigation. This work describes a concerted effort, where machine learning (ML) is used to accelerate discrete-event simulation. First, an ML-based instruction latency prediction framework that accounts for both static instruction properties and dynamic processor states is constructed. Then, a GPU-accelerated parallel simulator is implemented based on the proposed instruction latency predictor, and its simulation accuracy and throughput are validated and evaluated against a state-of-the-art simulator. Leveraging modern GPUs, the ML-based simulator outperforms traditional simulators significantly.

1. Introduction

Adopted extensively in computer architecture research and engineering, cycle-accurate discrete-event simulators (DES) enable new architectural ideas, as well as design space exploration. DES is composed of distinct modules that mimic the behavior of different hardware components. On certain events (e.g., advancing a cycle), these individual components and their interactions are simulated to imitate the behavior of processors. Unfortunately, DES is extremely computationally demanding, markedly diminishing its practicality and applicability at full system and application scales. Typical simulations using the state-of-the-art gem5 simulator [7] execute at speeds of hundreds of kilo instructions per second on modern CPUs, about four to five orders of magnitude slower than native execution. In this context, it would require extended periods of time to execute realistic applications that may contain trillions of instructions. To expand the practical limits of traditional simulation, design space exploration necessitates a multitude of simulations across various applications and design parameters under consideration.

Although simulation speed has steadily improved through statistical methods [40, 47], software engineering optimizations [36, 15, 29], and multi/many-core simulation parallelization [16, 35]. One fundamental limitation of these traditional simulators is they are intrinsically difficult to parallelize because of the heterogeneous nature of distinct components, frequent interactions between components, and irregular behaviors. As a result, existing parallel simulators focus on a

coarse parallelization strategy, where the simulation of individual cores is parallelized [16, 35]. These simulators have limited scalability and cannot leverage modern parallel accelerators, such as GPUs.

Recently, machine learning (ML) advances have led to remarkable achievements in many domains, and using ML for performance modeling is significant and growing. Considerable research has been done to predict application performance [14, 21, 22, 4, 5, 6, 27, 49]. The major limitation of these application-centric methods is they are program/input dependent, which means ML models need to be trained for distinct program and input combinations. As a result, their flexibility is limited compared to simulation-based approaches.

Ithemal [24] represents the closest related work to this effort, proposing a long short-term memory (LSTM) model to predict the execution latency of static basic blocks. However, Ithemal has three major limitations: 1) it targets a simplified processor model without branch prediction and cache/memory hierarchies; 2) it can only predict the performance of basic blocks with a handful of instructions, while real-world simulation executes billions or trillions of instructions; and 3) it simulates instructions at a pace of thousands of instructions per second, which is significantly slower than traditional simulators. As a result, Ithemal can neither simulate real-world processors nor applications.

This work tackles all of these problems to establish the first ML-based architecture simulator that can simulate realistic processors and application workloads. We introduce SIMNET, a novel instruction-centric simulation framework that decomposes program simulation into individual instruction latency and uses tailored ML techniques for instruction latency prediction. Program performance is obtained by combining the latency prediction results of all executed instructions. Figure 1 shows the SIMNET overview. SIMNET achieves noticeably higher simulation throughput while maintaining the same level of simulation accuracy because: 1) it abstracts the simulated processor as a whole and eliminates the need to simulate individual components within the processor, and 2) ML inferences are highly parallel, and state-of-the-art accelerators (e.g., GPU; TPU [17]) and software infrastructures [28, 3, 43] are well optimized for such tasks. This work’s contributions to the science and practice of simulation include:

- We propose an ML framework to predict instruction latency accurately (Section 2). The proposed framework accounts for both static instruction properties and dynamic proces-

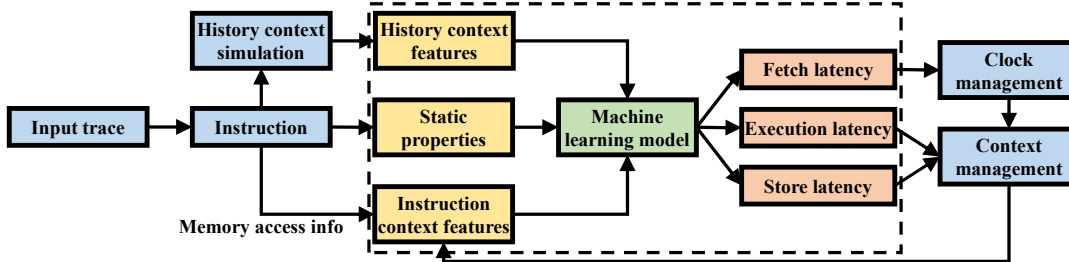


Figure 1: ML-based simulation framework. The ML-based instruction latency predictor is shown in green, and its input and output are in yellow and orange, respectively (Section 2). Other simulator components are in blue (Section 3).

- sor behaviors, and extensive ML models are evaluated to balance between the prediction accuracy and speed.
- We propose an instruction-centric architecture simulator that is built upon ML-based instruction latency predictors (Section 3). Evaluated using a realistic benchmark suite and on full microprocessor architectures, we demonstrate that the proposed approach simulates programs faithfully compared with the discrete-event simulator it learns from. To the best of our knowledge, the proposed framework is the first of its kind and could set the stage for developing alternative tools for architecture researchers or engineers.
 - We also prototype a GPU-accelerated ML-based simulator (Section 3.4). It improves the simulation throughput up to $37.1\times$ compared to its traditional counterpart.

Scope of Work. This paper focuses on simulating **out-of-order superscalar CPUs**, which employ technologies such as multi-issue, out-of-order scheduling, and speculative execution to exploit instruction-level parallelism. We posit the proposed simulation methodology also is applicable to other processor architectures, which usually are less challenging to simulate. In addition, we constrain the scope to the **prediction of program performance** and **single-thread program simulation**, leaving multiple-thread/program simulation for future work. Traditional simulators also produce additional metrics other than performance, such as energy consumption. While it is reasonable to assume the proposed method is applicable to such prediction as well, these metrics are not considered in this work.

2. ML-based Latency Prediction

This section describes the proposed ML-based instruction latency prediction framework as shown inside the dashed box of Figure 1.

2.1. Factors that Determine Instruction Latency

Successful instruction latency prediction by an ML model is contingent upon capturing all factors that impact latency in its design and implementation. These factors can be summarized into three categories.

Static Instruction Properties. These properties describe the basics of an instruction, including the operation types, source/destination registers, etc. They guide how an instruction is executed in a processor. For instance, the type of

instruction determines its computation resource (e.g., function units; register files) and synchronization requirements (e.g., memory barriers). These static properties can be extracted from the instruction encoding directly.

Dynamic Processor States. Besides its static properties, the latency of an instruction largely depends on the states of all processor components (e.g., register file; caches) at its execution time. We refer to these states as *contexts* and further distill them into two categories.

Instruction Context: Many contexts relate to other concurrently running instructions in the processor, referred to as *instruction context* in this paper. For example, whether the desired execution unit is available depends on how many co-running instructions have the same operation type, and if a source register can be read immediately depends on whether the previous instruction that writes the same register has finished. We argue that instruction context can be determined given all concurrently running instructions, named *context instructions* in this paper. The processor capacity decides the maximal number of context instructions.

History Context: The remaining hardware contexts depend on events that happened in the long-term execution history. Cache, translation lookaside buffer (TLB), and branch predictor states belong to this category. For example, whether a memory load hits in the L2 cache depends on when the same cache line was last accessed, and branch prediction results hinge on the branch execution history. Traditional simulators employ lookup tables (e.g., cache tag array; branch target predictor) to keep track of such states. We refer to them as *history context*.

2.2. Framework Formulation

With these impact factors, we are ready to build an instruction latency prediction framework. The framework aims to balance between two competing goals: to predict instruction latency *accurately* and *swiftly*. An ML-based instruction latency predictor (the green box in Figure 1) is the center of the framework, which captures the impact of input features. Its inputs (yellow boxes) take into account the aforementioned impact factors. Table 1 summarizes the input features, which are divided into three categories based on which impact factor they model as introduced below.

Modeling Static Instruction Properties. The second row of

Impact Factor	Features
Static properties	13 operation features (function type, direct/indirect branch, memory barrier, etc.); 14 register indices (8 sources and 6 destinations)
Instruction context	27 static properties; 14 history context features; 1 residence latency; 1 execution latency; 1 store latency; 5 memory dependency flags to indicate if it shares the same instruction/data address/cache line/page with the current instruction
History context	1 branch misprediction flag; 1 fetch level; 3 fetch table walking levels; 2 fetch caused writebacks; 1 data access level; 3 data access table walking levels; 3 data access caused writebacks

Table 1: Input features for various instruction latency impact factors.

Table 1 lists the static instruction properties used as the input features of the ML model, including 13 operation flags and 14 source and destination register indices. They are well known to computer architects.

Modeling Instruction Context. To account for the impact of concurrently running instructions, the key is to model their *relationships* with the to-be-predicted instruction. Such relationships include resource competition, register dependency, and memory dependency. We call these concurrently running instructions, *context instructions*. Formally, the context instructions are those instructions present in the processor when a particular instruction is about to be fetched. In theory, instructions issued after the current instruction also can influence its execution. However, these cases are rare, and we only include previous instructions for practicality. The third row of Table 1 shows input features per context instruction.

For resource competition and register dependency, it is sufficient to provide the static properties of context instructions (i.e., their operation features and register indices). The ML model is responsible for deducing the resource competition using their operation features and the register dependency by comparing register indices.

To model the memory dependency (including instruction fetch and data access), one solution is to provide memory access addresses as parts of input features. Unlike register indices, memory access addresses spread across a much wider range in a typical 64-bit address space. Thus, having addresses as input would slow down the ML model prediction speed. Instead, we extract the memory dependency by explicitly comparing the memory access addresses of the current instruction with those of context instructions and generate several *memory dependency flags* as input features. For example, we compare their program counters (PCs) to identify if they fall into the same instruction cache line. This PC dependency flag presumably helps with fetch latency prediction as instructions that share the same instruction cache line can be fetched together. Similarly, there are dependency flags to indicate if data accesses share the same address, cache line, and page.

In addition, we introduce several features to capture the temporal relationship between instructions. Particularly, we include the number of cycles it has stayed in the processor (i.e., residence latency), how long it takes to complete execution (i.e., execution latency), and the memory store latency (i.e., store latency) if applicable. The latter two are provided by the ML model output, which will be introduced shortly. The latency of context instructions is useful to predict the latency

of the current one. For example, when an instruction follows a mispredicted branch, its fetch latency is decided by the execution latency of the branch.

Modeling History Context through Simplified Simulation.

History context reflects the hardware states that depend on long-term historical events, and it includes caches, TLBs, and branch predictors. It is impractical to either capture the history context within the ML model or directly have it as the input because it includes a huge amount of information. Considering a 2MB cache with 64B cache lines as an example, we will need $\sim 5B$ per cache line to store its address tag, etc. Totally, a 2MB cache requires storing at least $2MB \div 64B \times 5B = 160KB$ of information to simulate it accurately. The total history-context-related information is much larger given all history context. It is prohibitively expensive and inefficient to allow the ML model to handle such large amounts of information directly.

Fortunately, the majority of history context impacts can be captured using a small number of intermediate results. For a memory access, the cache/TLB level in which it gets hit roughly determines its latency. Similarly, whether or not a branch target is predicted correctly determines the impact of a branch.

Therefore, we propose to simulate history context components explicitly to obtain these intermediate results (i.e., *history context simulation*), which are passed to the ML model as input features. History context simulation greatly alleviates the burden on ML models. As shown in the last row of Table 1, a branch misprediction flag is obtained for a branch instruction. An *access level* feature is used for each memory access to indicate which level of the cache/TLB hierarchy satisfies the request. All instructions require fetch access and fetch table walking levels, and load/store instructions need data access and data table walking levels, e.g., a load request that hits in the L2 cache has a level of 2. The numbers of cache writebacks generated are also included in input features to capture their impacts.

Note that obtaining these intermediate results mostly involves table lookups (e.g., cache tag array; branch direction predictor). Detailed structures, such as pipeline and miss status history register (MSHR), are not needed in the history context simulation, whose impacts are captured by the ML model. Therefore, the history context simulation is lightweight and has negligible impact on the overall performance.

ML Model Input Summary. In total, each context instruction has 50 features, and the to-be-predicted instruction has 47 features. For alignment purposes, we pad the to-be-predicted

instruction features with three zeros, to have an equal number of 50 features. Together, the ML model input includes $50 \times (\# \text{ context instructions} + 1)$ features. While it is common to adopt one-hot encoding for individual input features, we choose not to do so for smaller input size and faster prediction speed.

ML Model Output. In Figure 1, the ML model is designed to predict three types of latency per instruction: fetch, execution, and store. Fetch latency represents how long an instruction needs to wait to enter the processor after the previous instruction is fetched. It is affected by both its instruction fetch request and context instructions (e.g., when it follows a mispredicted branch). Execution latency represents the time interval from when an instruction is fetched to when it finishes execution and is ready to retire from the reorder buffer (ROB). Note it is different from the ROB retire latency because the ROB retires instructions in order. For store instructions, they write memory after being retired from the ROB. The store latency is used to represent the latency from when a store instruction is fetched to when it completes memory write (i.e., when it is ready to retire from the store queue (SQ)).

2.3. Neural Network Architecture

Given the input and output, we train various ML models to learn their connections by capturing the architectural impact.

Sequence-Oriented Models. The ML model input includes a sequence of instructions (i.e., to-be-predicted instruction and context instructions), similar to word sequences in the case of natural language processing (NLP). Therefore, an attractive option is to apply models designed to process sequences, such as recurrent neural networks [34], LSTM [13], and Transformer [44], for instruction latency prediction. Ithemal [24] follows this strategy and adopts LSTM to predict basic block latency. However, these models are more computational intensive, which will be illustrated in Section 2.5, resulting in low simulation throughput. Moreover, they are designed to account for the impact of longer sequences because every word that appears earlier matters to the semantic meaning of an article or speech. In the instruction latency prediction case, the number of context instructions is limited by the processor capacity, and we do not need to consider instructions that have exited the processor.

Deep Convolutional Neural Network (CNN) Models. Deep CNN models have shown great success in computer vision [20, 12, 42], where convolution kernels learn and recognize the spatial relationship between pixels. In our instruction latency prediction setting, convolution can help learn the relationship among input instructions. CNNs are less computational demanding than sequence-oriented models and fully connected networks. Another benefit of CNN is it has significantly less to-be-learned parameters and thus is easier to converge in training. Therefore, we choose CNNs for our instruction latency predictors.

Figure 2 illustrates the proposed CNN architecture. $Inst_0$

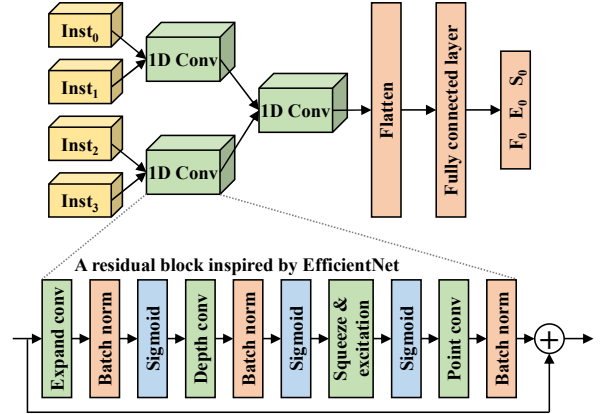


Figure 2: Neural network architecture illustration.

represents the instruction to be predicted, and the ML model outputs F_0 , E_0 , and S_0 , which are its predicted fetch, execution, and store latency, respectively. Without loss of generality, Figure 2 shows three context instructions, $Inst_{1,2,3}$.

We organize input instructions in a one-dimensional (1D) array by their execution order and have their features as channels, per CNN terminology. As introduced in Section 2.2, every instruction includes 50 features. Using computer vision as an analogy, instructions correspond to pixels, except they are 1D instead of two-dimensional, and instruction features correspond to pixel color channels. This input organization facilitates convolutional operations to reason the relationship between instructions. Again, it is analogous to reasoning the shape composed by pixels in computer vision.

We organize the convolutional layers in a hierarchical way, where the first layer captures the relationship between temporally adjacent instructions, and subsequent layers integrate the impact of further away instructions. In Figure 2, the impact of $Inst_1$ to $Inst_0$ is captured in the first layer, and the impact of $Inst_3$ is incorporated in the second layer. This hierarchical design prioritizes the impact of temporally closer context instructions while penalizing the influence of more distant instructions. For instance, if a source register of $Inst_0$ is the destination register of both $Inst_1$ and $Inst_3$, $Inst_0$ only has to wait for $Inst_1$ where a true read after write dependency exists.

In our default design, each convolution layer includes a convolution operation followed by an activation operation. An alternative is to use a residual block as shown at the bottom of Figure 2, which facilitates to increase the depth of CNNs [12]. In this work, we design a residual block with architecture inspired by the state-of-the-art computer vision model, EfficientNet [42, 41].

Empirically, we find the following CNN design principles work well for instruction latency prediction. First, the inputs of different convolutional operations have no overlap in contrast to computer vision CNNs. For example, we do not convolve $Inst_1$ and $Inst_2$ in Figure 2. In this way, the impact of a context instruction is integrated only once. Second, a convolution kernel size of 2 is always used to account for only two adjacent

inputs, which reduces the complexity. Combined with the first principle, it means all convolutional layers have the uniform kernel and stride size, 2. Our experiments demonstrate that these principles work well across different architecture configurations and eliminate the need to explore the design space of CNNs.

The output of the last convolutional layer is flattened then used as the input of two fully connected layers. At the end, the model outputs the predicted fetch, execution, and store latency of Inst_0 . We adopt the commonly used rectified linear unit (ReLU) as the activation function of both the convolutional and fully connected layers.

From Output to Latency. There are two ways to convert the ML model output to the latency prediction results. In a *regression* model, the model output is directly used as the predicted latency. One inherited issue for the regression latency prediction model is its inability to distinguish between small latency differences. The impact may be minimal when a latency of 1000 cycles is predicted to be 1001 cycles, but the error could be significant for small latency (e.g., 0 cycle predicted to be 1). Because the fetch latency is 0 or 1 cycle in most cases, this drawback is particularly critical for its prediction.

A *classification* model could help to better distinguish between close latency values, where every latency value corresponds to a class, and the ML model predicts which class has the largest probability. However, because the latency could be up to several thousands of cycles, a pure classification scheme will significantly increase the output size and, thus, the computational overhead. Another problem of a pure classification scheme is it is difficult to train such a model because large latency samples appear rarely in the training set.

As it is quite expensive to have a class for each possible latency value, we propose a *hybrid* scheme which uses classification for latency that appears frequently and regression for others. Naturally, small latency appears more frequently. Taking the fetch latency prediction as an example, we classify them into 10 classes in the hybrid scheme. Cycles 0 to 8 have dedicated classes (c_0, \dots, c_8), while another class is used to represent cycles that are larger than 8 ($c_{>8}$). The proposed model outputs the probability of each class. It also outputs a direct prediction result l as in the regression model. On a prediction, we first check which class has the largest probability. If it is one among c_0, \dots, c_8 , the corresponding latency is predicted. Otherwise, l is used as the predicted latency. Similar procedures are used to predict execution and store latency.

2.4. Dataset and Training

Due to their data-driven nature, acquiring a sufficiently large training dataset is necessary for the success of ML-based approaches. Fortunately, it is convenient to engage existing simulator infrastructures to acquire a dataset for standard *supervised* training. We modify gem5 [7] to dump instruction execution traces, which then are used to generate ML training/validation/testing datasets.

Table 2 shows the processor configurations that ML models

Parameter	Default O3CPU	A64FX
Core	3-wide fetch, 8-wide out-of-order issue/commit, bi-mode branch predictor, 32-entry IQ, 40-entry ROB, 16-entry LQ, 16-entry SQ	8-wide fetch, 4-wide out-of-order issue/commit, bi-mode branch predictor, 48-entry IQ, 128-entry ROB, 40-entry LQ, 24-entry SQ
L1 ICache	48KB, 3-way, LRU, 4 MSHRs	64KB, 4-way, LRU, 8 MSHRs
L1 DCache	32KB, 2-way, LRU, 16 MSHRs, 5-cycle latency	64KB, 4-way, LRU, 21 MSHRs, 8-cycle latency, 8-degree stride prefetcher
I/DMMU	2-stage TLBs, 1KB 8-way TLB caches with 6 MSHRs	2-stage TLBs, 1KB 4-way TLB caches with 6 MSHRs
L2 Cache	1MB, 16-way, LRU, 32 MSHRs, 29-cycle latency	8MB 16-way, LRU, 64 MSHRs, 111-cycle latency

Table 2: Simulated processor configurations.

learn from. The default O3CPU resembles a classic superscalar CPU. We also train models to learn the Fujitsu A64FX CPU deployed in the current top-ranked supercomputer, Fugaku [48, 37], which represents the state-of-the-art CPU. We obtain the official gem5 configurations of A64FX at [2]. Both processors support the ARMv8 instruction set architecture (ISA), and benchmarks are compiled using gcc 8.2.0 under the O3 optimization level. The full system simulation mode of gem5 is employed with Linux kernel 4.15.

We use the default O3CPU configuration for most of our experiments, while Section 4.4 will present the results for the A64FX configuration. Under the default O3CPU configuration, there are, at most, 110 context instructions. Therefore, the ML model input has $50 \times (1 + 110) = 5550$ features.

Benchmark. Theoretically, any program can be run on the modified gem5 to collect the ML dataset, and we can acquire an unlimited amount of data. We choose to use the SPEC CPU2017 [8] benchmark suite in practice because it includes a wide range of applications, which should lead to a sufficient coverage of instruction execution scenarios. Out of 21 SPEC CPU2017 benchmarks compiled and run in our experimental environment successfully, we select the first four to generate the ML training/validation/testing dataset and leave the remaining 17 benchmarks for simulation testing. Table 3 shows these benchmarks. The default ref inputs are used, and one billion instructions are simulated from the beginning for each benchmark to collect traces. Notably, we use the SPECrate benchmarks while excluding SPECspeed ones due to their similarity.

Because the ML model predicts the latency at the instruction level and most benchmarks use a variety of instructions, benchmark selection for the training set is not critical and can be almost arbitrarily decided. We expect reasonable ML prediction accuracy as long as we collect ample data to cover enough instruction and context scenarios. Section 4.5 will evaluate the impact of training dataset size on prediction accuracy.

ML Data Processing. In the modified gem5, each instruction is assigned with three timestamps to record its respective fetch, execution, and store latency. While the fetch latency stamp is updated in the instruction fetch unit, the execution and store latency stamps are updated in the ROB and SQ, respectively. After all latency of an instruction is recorded, gem5 dumps it

Type	ML	Simulation
INT	500.perlbenc, 502.gcc	505.mcf, 523.xalancbmk, 525.x264, 531.deepsjeng, 548.exchange2, 557.xz, 999.specrand_i
FP	503.bwaves, 508.namd	507.cactuBSSN, 519.lbm, 521.wrf, 526.blender, 527.cam4, 538.imagick, 544.nab, 549.fotonik3d, 554.roms, 997.specrand_f

Table 3: Benchmarks for ML and simulation.

to a trace file.

The instruction traces output by gem5 require several steps of processing before they can be used for ML. First, for each instruction, we find and associate its context instructions based on the timestamps to form a *sample*. Second, many samples may be alike because the same scenarios can appear repeatedly during the execution of benchmarks. We eliminate such duplication to reduce the dataset. Finally, we convert the dataset to a format acceptable by the ML framework used: PyTorch 1.7.0 [28]. On the four SPEC CPU2017 benchmarks used for the ML dataset, the modified gem5 generates 489GB of original trace data. After processing, we obtain a 33GB compressed dataset with 71 million samples, among which roughly 90% of them are used for training, 5% for validation, and 5% for testing.

Training. We train various models using the Adam optimizer in PyTorch 1.7.0 [19]. We use a learning rate of 0.001 and no weight decay or momentum. Every model is trained for 200 epochs, and the validation set is used to select the model with the lowest loss. Our ML training hardware platform is an NVIDIA DGX A100 system [1]. It includes eight NVIDIA A100 GPUs connected through NVLink 3.0 and NVSwitch, and each is equipped with 40GB HBM that supports 1.5 TB/sec peak bandwidth. Tensor cores in an A100 GPU enable a peak performance of 156 TFlops for Tensor Float 32 operations. The DGX A100 system’s high computing and memory throughput make it ideal for ML training and inference. Training a model takes 150 ~ 600 A100 GPU hours depending on its complexity. The total training time will be 5 ~ 19 hours with 32 GPUs.

2.5. Model Evaluation

We evaluate an array of ML models for instruction latency prediction, and the left part of Table 4 compares their prediction accuracy. For CNNs, C and F represent the respective convolutional and fully connected layers, and RB denotes the residual block depicted at the bottom of Figure 2. The prefix number represents the number of particular type layers. For example, the 3C+2F model is composed of three convolutional layers followed by two fully connected layers. We also evaluate two sequence-oriented models, including an LSTM model that is similar to Ithema [24] and a Transformer model that uses attention mechanisms [44]. Due to space limitations, we only list a small fraction of models that have been evaluated.

For every model, we show two prediction errors for each latency type. E_c represents the average absolute cycle difference between the prediction and truth, i.e., $E_c = \text{AVG}(|f_\theta(x_i) - y_i|)$.

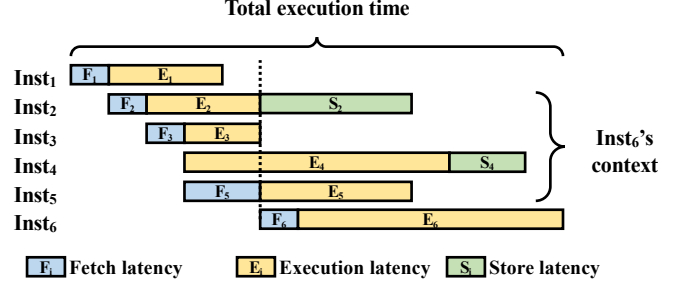


Figure 3: From instruction latency to program execution time.

E_p is calculated by dividing the total absolute cycle differences by the total truth cycles, i.e., $E_p = \frac{\sum |f_\theta(x_i) - y_i|}{\sum y_i}$. As we will see soon in Equation 1, E_p of fetch latency is a useful indicator of the program simulation error because $\sum y_i$ is close to the true simulation time. Section 3.3 will discuss the relationship between latency prediction accuracy and program simulation accuracy in detail. Of note, the normalized error metric is not applicable here because the fetch and store latency (i.e., non stores) is often 0.

Table 4 affords several observations. First, we note that the prediction accuracy of CNNs improves with the number of layers, which demonstrates the necessity of a **deep** neural network. Particularly, 7RB+2F with residual blocks achieves the best accuracy, while the simplest 2F model’s fetch latency E_c is more than 10 times larger. Second, the **hybrid** scheme helps reduce prediction errors, from 0.50 to 0.19 for fetch latency’s E_c under 7C+2F, while barely increasing the computation complexity. We notice that the hybrid 7C+2F model makes correct fetch latency predictions in 96% of cases. In comparison, the regression 7C+2F model predicts 68% of fetch latency correctly, which demonstrates that classification is helpful to predict latency with small values.

The computational overhead of CNN models varies between 8 ~ 93 millions of multiplications per inference. They represent different trade-off points between accuracy and computation overhead. Although they seem to be higher than that of traditional simulators, these computations are performed very efficiently on modern accelerators, such as GPUs and TPUs, which allows SIMNET to speedup simulation significantly and will be introduced later.

Compared with CNN models, both LSTM and Transformer models show lower prediction accuracy while incurring much larger computational overhead. Transformer models are especially expensive due to the attention computation [44]. Although there are spaces to improve their accuracy, it often requires the adoption of deeper and wider networks which come along with larger overhead. This demonstrates that CNNs are more efficient at instruction latency prediction under a constrained computation budget.

Model	Output	MFlops	Fetch lat.		Execution lat.		Store lat.		Benchmark simulation error					
			E_c	E_p	E_c	E_p	E_c	E_p	mcf	cactuBSSN	roms	xz	range	abs. avg.
2F	reg	5.69	1.68	57%	3.66	4.3%	2.38	8.4%	21%	16%	28%	20%	[-0.97%, 28%]	18%
3C+2F	reg	8.08	0.76	26%	2.11	2.5%	1.04	3.7%	0.81%	0.59%	1.5%	-0.84%	[-6.6%, 5.2%]	1.9%
5C+2F	reg	21.37	0.48	16%	1.29	1.5%	0.73	2.6%	0.47%	1.7%	1.1%	-0.05%	[-4.6%, 5.5%]	2.0%
7C+2F	reg	50.77	0.50	17%	1.25	1.5%	0.64	2.3%	-2.4%	-0.37%	-1.4%	-4.7%	[-8.7%, 6.3%]	2.5%
7C+2F	hyb	50.8	0.19	6.2%	1.11	1.3%	0.62	2.2%	-0.63%	0.43%	1.3%	-5.5%	[-6.3%, 11%]	2.3%
7RB+2F	hyb	93.32	0.15	5.1%	0.96	1.1%	0.52	1.8%	-0.8%	-1.0%	-0.1%	-2.7%	[-2.7%, 0.78%]	0.96%
LSTM	hyb	118.84	0.57	19%	3.27	3.8%	1.29	4.5%	-1.9%	-1.5%	-0.45%	-6.2%	[-6.2%, -0.38%]	2.4%
Transformer	hyb	1185	0.49	17%	2.06	2.4%	0.88	3.1%	2.1%	1.4%	2.3%	0.39%	[-0.70%, 17%]	2.4%

Table 4: Instruction latency prediction and program simulation accuracy of various ML models. Output indicates if it is a regression model (reg) or hybrid model with classification (hyb). MFlops indicates how many millions of multiplications are required for one inference. Each benchmark is simulated for 10 million instructions.

3. ML-based Simulation

3.1. From Instruction Latency to Program Performance

With the ML-based instruction latency predictor, another key question is how to use it to simulate the program performance. Figure 3 illustrates how to calculate program execution time using instruction latency, leveraging the fact that instruction fetch and instruction retire from ROB and SQ happen in order. Note that the fetch latency could be 0 in cases when multiple instructions are fetched together (e.g., $Inst_4$). We observe the execution time \mathcal{E} of a program can be computed as

$$\mathcal{E} = \left(\sum_{i=1}^n F_i \right) + \Delta, \quad (1)$$

where n is the total number of simulated instructions, F_i represents the fetch latency of the i th instruction, and Δ is the amount of time from when the last instruction is fetched to when all instructions exit the processor. When n is large enough, the total execution time is dominated by the accumulated fetch latency, and Δ is negligible. This equation provides the foundation for the proposed instruction-centric simulator.

3.2. Simulator Implementation

Based on Equation 1, we develop a trace-driven simulator. The simulator goes through every instruction to predict its latency and outputs the program performance upon completion. The modified gem5 is used to generate input traces, which include instruction properties extracted by functional simulation, and history context simulation results, including memory access levels and branch misprediction flag.

Context Management. As introduced in Section 2.2, the ML predictor requires the features of context instructions as part of its input. Therefore, SIMNET needs to keep track of context instructions. For example, in Figure 3, when $Inst_6$ is about to be fetched (vertical black-dotted line), $Inst_1$ has retired, and $Inst_{2\sim5}$ are still in the processor based on their execution and store latency. Therefore, $Inst_{2\sim5}$ are the context instructions of $Inst_6$. To this end, we employ two first-in-first-out (FIFO) queues, *processor queue* and *memory write queue*, to keep track of context instructions that stay in the processor and their features. They roughly correspond to the ROB and SQ in an out-of-order processor but are not exactly the same. The two major differences are that the processor queue includes instructions in the frontend, while ROB does not, and a store

instruction enters the memory write queue after it retires from the processor queue.

After the simulator reads one instruction from the input trace, the ML predictor is invoked to predict its latency. Then, it enters the processor queue with the residence latency initialized to 0. When it retires from the processor queue is determined based on its predicted execution latency and other simulation constraints (e.g., it must obey the in-order retirement and retire bandwidth). A non-store instruction exits the simulator when it retires from the processor queue. For a store instruction, it will enter the memory write queue. Similarly, when an instruction retires from the memory write queue is decided based on its predicted store latency, and it will exit the processor at that time. Much like real processors, the retire bandwidth of a processor queue is set according to that of the ROB, and the memory write queue can retire any number of instructions from its tail.

Clock Management. The simulator employs `curTick` to record the total number of simulation cycles, which is updated whenever a prediction completes. When the predicted fetch latency is larger than 0, it is added to `curTick` so that the counter always points to the time when the current instruction enters the processor. In this case, we also increase the residence latency of all context instructions by the predicted fetch latency to update the time that they have remained in the processor. When the residence latency of an instruction is larger than its execution latency, it is ready to retire from the processor queue. Similarly, an instruction is ready to retire from the memory write queue when its residence latency exceeds its store latency.

After the last instruction in the input trace is predicted, we continue advancing `curTick` until all instructions retire from the simulator. The final value of `curTick` represents the total execution time of the program, which is exactly the same as Equation 1.

3.3. Predictor Accuracy versus Simulation Accuracy

One crucial question that determines the feasibility of our instruction-centric simulation approach involves the relationship between the accuracy of the instruction latency predictor and that of the simulator built upon it. Intuitively, an accurate instruction latency predictor should lead to an accurate simulator. However, because previous prediction results are

used to construct the input of latter predictions through the instruction context, the relationship between the predictor’s and simulator’s accuracy is complicated.

To answer this question, the right side of Table 4 illustrates the program simulation error of various models compared with gem5. It includes the simulation errors for four selective benchmarks (due to space constraints). It also shows the error range and average absolute error for all 17 benchmarks. We simulate 10 million instructions for each benchmark from the beginning. The simulation error E_s is calculated as $(CPI_{SIMNET}/CPI_{gem5} - 1) \times 100\%$, and the average absolute error is $AVG(|E_s|)$. We observe the simulation error is below 3% for all models, except the simplest 2F model.

There are two reasons why SIMNET achieves accurate simulation. First, the processor pipeline is emptied every once in a while due to events such as branch misprediction during simulation. Upon these events, there are no context instructions, and the predicted latency does not rely on previous prediction results. As a result, the simulation accuracy gets calibrated on these events. Second, a well-trained ML model can self-correct its behaviors throughout the simulation because such self-correction often happens during a real processor’s execution. For example, assume one instruction I takes longer than it should and prevents the next instruction I_n from entering the processor earlier. When I_n enters, the processor pipeline is emptier than it should be, which results in faster execution of I_n . In such a scenario, I is executed slower, while I_n is executed faster. Together, the total execution time calibrates towards the right direction.

We have previously observed that deeper CNN models have better instruction prediction accuracy, but the improvement on instruction prediction accuracy does not convert to that on simulation accuracy until the most accurate 7RB+2F model. 7RB+2F achieves the best accuracy and narrowest error range across various models, and its average absolute simulation error is 0.96% across 17 benchmarks. These models represent a variety of **trade-off** points between accuracy and cost. While 7RB+2F is the most accurate model also with a high computational cost, 3C+2F achieves acceptable accuracy at a low cost.

Traditional simulator developers validate the simulator accuracy against the hardware that it intends to simulate. Usually, an error around 10% is considered to be acceptable. For example, ZSim reports an average IPC error of 9.7% against an Intel Westmere CPU [35], and [11] reports a 13% error of gem5 against an ARM Cortex-A15 system. Although we validate the accuracy of SIMNET against gem5 instead of real CPUs, we contend its average absolute error of $0.96 \sim 2.5\%$ is sufficient to gain confidence about simulation results because it allows SIMNET to achieve similar simulation accuracy compared with the simulator it learns from. Section 4.1 will further validate the simulation accuracy across execution phases.

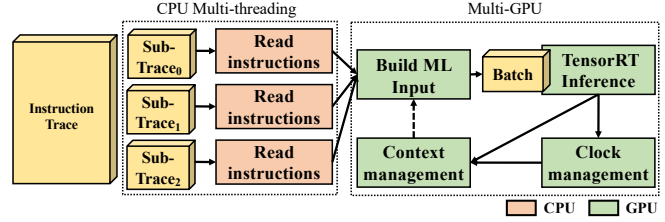


Figure 4: Parallel simulation framework.

3.4. GPU-accelerated Parallel Simulation

In our ML-based instruction latency predictor, the latency of an instruction depends on the predicted latency of previous instructions, i.e., the latency prediction of adjacent instructions is inherently sequential. This restriction limits the simulation speed, and the sequential SIMNET runs at a throughput of nearly 1k instructions per second. To improve the simulation speed/throughput, we seek to extract parallelism in the sequential simulation.

Parallel Simulation of Sub-traces. The primary idea is to break down the input instruction trace into multiple, equally sized continuous sub-traces and simulate sub-traces in parallel and independently. The drawback of this approach is that extra simulation errors are introduced when simulating head instructions of a sub-trace due to inaccurate contexts. Section 4.2 will show that such accuracy loss is negligible when each sub-trace is large enough.

Figure 4 shows the overview of parallel simulation. The design leverages CPU multi-threading to partition the input trace and transfer sub-trace instructions to the GPU memory. The remaining work is done by GPUs to capitalize on their high computational capacity and reduce communications between CPUs and GPUs.

GPU Acceleration. Both context and clock management are implemented on GPUs, and each sub-trace has separate copies of them. Particularly, each sub-trace has its own processor queue and memory write queue, as well as a `curTick` counter to record its number of cycles passed. After the ML model input is built independently for each sub-trace, we combine them into a single input to allow GPU-batched inferences. This process repeats until all instructions in a sub-trace are simulated. After all sub-traces complete their simulation, we sum up their `curTicks` to get the total execution time.

For ML model inferences, we use TensorRT [43], developed by NVIDIA for high-performance GPU deep learning inferences. It optimizes GPU memory allocations and supports reduced precision inferences. Compared with PyTorch, it provides roughly $4\times$ speedup.

In addition, this design can be scaled to multiple GPUs, where each GPU is responsible for a fraction of sub-traces. Section 4.2 will offer a detailed evaluation of simulation throughput.

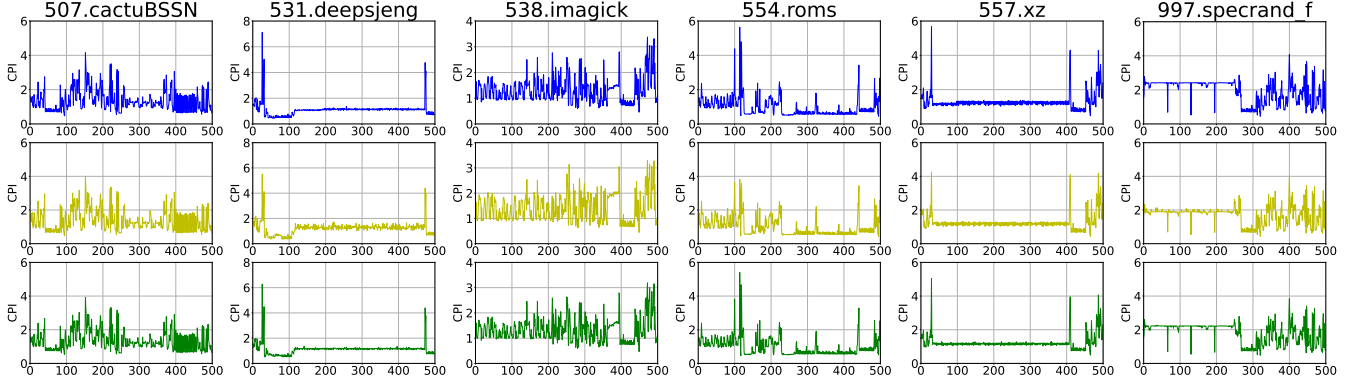


Figure 5: CPI variations during simulation. Each column represents a benchmark. The top row shows the gem5 simulation results, the middle row lists the 3C+2F results, and the bottom row features the 7RB+2F results.

4. Evaluation

We conduct simulation experiments on our training platform: the NVIDIA DGX A100 system equipped with eight A100 GPUs and an AMD EPYC 7742 64-core CPU.

4.1. Simulation Phase Validation

To verify the simulation accuracy with respect to execution phases, Figure 5 studies the cycle per instruction (CPI) variation under 3C+2F and 7RB+2F models for six representative benchmarks, including 997.specrand_f and 557.xz, where they show the largest simulation errors. Particularly, we calculate the average CPI for every 10k simulated instructions and plot these CPIs over a simulation length of 5M instructions (500 points in total). Overall, SIMNET’s CPI curves closely resemble those of gem5, especially those using 7RB+2F. For 538.imagick, 3C+2F’s CPI diverges from that of gem5 between point 360 and 390, while 7RB+2F’s CPI is more similar. We also observe that a period of inaccurate simulation does not impact the simulation accuracy of the time periods that follow. For instance, although 3C+2F does not simulate the first half of 997.specrand_f accurately, its CPI curve is almost identical to that of gem5 in the second half. This is because the simulation error gets calibrated when the processor pipeline is empty. On average, the absolute phase simulation errors across 17 benchmarks are 3.5% for 3C+2F and 1.8% for 7RB+2F. These results show that SIMNET not only can predict the overall performance well, but it also generates insights, such as identifying which execution phases are performance bottlenecks.

4.2. Parallel Simulation

Accuracy. Because the parallel simulator partitions the input trace into multiple sub-traces, there is simulation accuracy loss across sub-trace boundaries. Figure 6 studies how the overall simulation accuracy varies with the number of instructions per sub-trace. It reports the average absolute errors when simulating 100M instructions for 17 benchmarks using three representative models. 7RB+2F cannot have sub-traces that are smaller than 12k instructions because the GPU memory cannot accommodate too many sub-traces. As the results show,

the simulation error generally decreases with an increasing number of instructions per sub-trace.

Throughput. We evaluate the simulation throughput of parallel SIMNET in terms of million instructions per second (MIPS). Figure 7 evaluates the average throughput across 17 benchmarks with various numbers of sub-traces using the same three models. Increasing the number of sub-traces enables SIMNET to utilize both CPU and GPU resources more efficiently until it saturates these resources. 7C+2F enjoys significant throughput improvement until 32k sub-traces, and the lightweight 3C+2F continues benefiting from more sub-traces. Limited by the GPU memory capacity, we cannot evaluate 3C+2F beyond 64k sub-traces or 7RB+2F beyond 8k sub-traces.

Figure 8 assesses the throughput scalability of SIMNET with multiple GPUs, where the horizontal black-dotted line marks the gem5 simulation throughput. As ML inferences take a significant portion of time in SIMNET, using multiple GPUs improves both the inference and simulation throughputs. SIMNET achieves near-linear speedup with the number of GPUs. With eight GPUs, it achieves 7.35, 5.59, and 0.68 MIPS with the 3C+2F, hybrid 7C+2F, and 7RB+2F models, respectively. Correspondingly, this represents 37.12 \times , 28.22 \times , and 3.44 \times improvement over gem5. We can further scale SIMNET to distributed systems easily for higher throughput.

History Context Simulation Overhead. History context simulation can achieve ~ 100 MIPS throughput because it only requires simplified results, such as cache access levels, where simulating address tag comparison and replacement is sufficient. Therefore, its overhead is negligible.

4.3. Impact of Features

Figure 9 evaluates the contribution of each input feature to the ML model output using the SHapley Additive exPlanation (SHAP) method [23]. SHAP computes Shapley values [39] using the coalitional game theory. Shapley value is the average marginal contribution of a feature value across all possible coalitions. We take the average of absolute Shapley values on training samples for each feature to produce feature attribution scores. Figure 9a and 9b summarize the attribution scores of to-be-predicted instructions and context instructions separately.

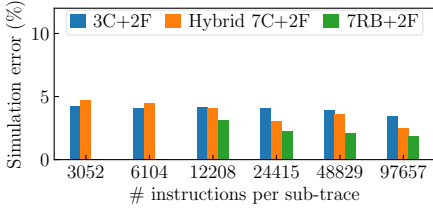


Figure 6: Average parallel simulation errors with various sub-trace sizes.

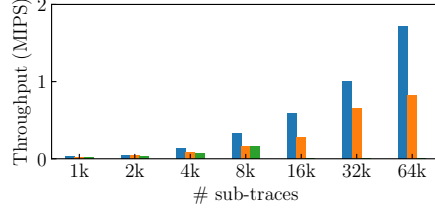


Figure 7: Simulation throughput with different sub-trace numbers.

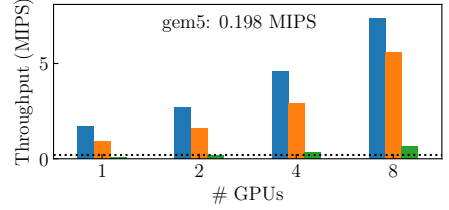


Figure 8: Simulation throughput with multiple GPUs.

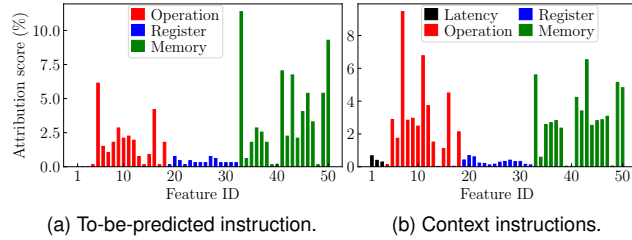


Figure 9: Feature attribution scores.

We categorize the 50 features into latency, operation, register, and memory. Memory and operation features generally have more impacts on the prediction results. The most influential feature of to-be-predicted instructions is the fetch access level because the fetch latency depends on it. For context instructions, the branch misprediction flag has the largest attribution score as mispredicted branches need to flush the processor pipeline.

4.4. Architecture Variation

We also evaluate the effectiveness of SIMNET under the A64FX configuration. Because A64FX can accommodate more instructions, it has up to 209 context instructions, and we train a hybrid 8C+2F model to incorporate more context instructions. Note that no hyperparameter tuning is performed to simulate A64FX. Compared with results under the default O3CPU configuration in Table 4, the A64FX model achieves a similar average absolute program simulation error of 2.2% across 17 benchmarks, which demonstrates that SIMNET also can effectively simulate more complex CPU architectures.

4.5. Impact of Training Dataset Size

We also generate a large ML training dataset using 15 SPEC CPU2017 benchmarks instead of four. With the hybrid 7C+2F model, using the large dataset reduces the average simulation error from 2.3% to 1.6%. We conclude that the smaller dataset is enough to train accurate models and also requires less training time.

4.6. Use Scenarios

SIMNET can be applied in many computer architecture research and engineering scenarios. First, most recent computer architecture efforts focus on caches or branch predictors because other microarchitecture components are sophisticated. In such scenarios, pre-trained ML models can be directly applied as caches and branch predictors are modeled in history context simulation, and no additional training

	Simulated speedup			Relative error range	
	gem5	3C+2F	7RB+2F	3C+2F	7RB+2F
BiMode_1	10.4%	11.2%	9.9%	[-2.7%, 3.7%]	[-1.7%, 1.4%]
TAGE-SC-L	12.3%	13.7%	12.4%	[-4.0%, 4.5%]	[-0.7%, 1.8%]

Table 5: Simulated speedups of various branch predictors.

is required. Second, when studying other microarchitecture parameters (e.g., ROB size) or novel components, different parameter/configuration choices can be included in the input of the ML model, so training a single model once is sufficient to study all variations. We illustrate these two points via three use cases. Computer architects typically use simulators to evaluate the relative speedup when altering certain parameters/components. Therefore, we evaluate the relative accuracy of SIMNET to compare with gem5 in these use cases.

Branch Predictor Study. We compare the simulated performance of two branch predictors using gem5 and SIMNET, including a large bi-mode branch predictor (BiMode_1) and the recently proposed TAGE-SC-L [38]. The implementation of branch predictors in gem5 is used in SIMNET’s history context simulation to generate branch misprediction flags for ML models’ input. Table 5 shows the simulated average speedups across 17 SPEC benchmarks, where the performance is normalized to that of a baseline bi-mode branch predictor. We observe that the average speedups obtained using SIMNET are similar to those using gem5. Moreover, the right side of Table 5 shows the speedup error ranges of individual benchmarks compared with gem5 results. We observe that SIMNET also predicts the speedups of individual benchmarks well, especially under 7RB+2F.

L2 Cache Size Exploration. We also simulate the performance impact of L2 cache sizes using gem5 and SIMNET. Recall that changing cache sizes does not require model training because caches are modeled in history context simulation. Similar to the branch predictor case, SIMNET accurately simulates the relative speedup under different cache sizes, and the average error against gem5 is 0.8%.

ROB Size Exploration. In this experiment, the ML model input includes the ROB size as an additional feature to account for its impact. The training data are generated by running the same four SPEC benchmarks in gem5 under various ROB sizes. We train a 3C+2F model to study the impact of ROB sizes. Again, the simulation results of SIMNET and gem5 agree with each other. For example, the average performance improvement when increasing the number of ROB entries from 40 to 80 and 120 is 1.2% and 1.4% under gem5. Using

SIMNET, the corresponding speedups are 1.1% and 1.5%, which are very similar.

5. Related Work

ML for Latency Prediction. Ithemal [24] uses LSTM models to predict the execution latency of static basic blocks. The instructions within a block are fed into the model in the form of assembly, such as words in NLP. On top of Ithemal, Diff-Tune [33] trains a differentiable ML performance model to configure the simulator parameters to closely resemble a target architecture. These methods pose limits as they do not consider dynamic execution behaviors, such as memory accesses and branches, which have significant impacts on program performance. They also target basic blocks with a limited number of instructions. As a result, they are not applicable to a computer architecture simulator that needs to simulate realistic processors and billions/trillions of instructions.

ML for Application Performance Prediction. Ipek *et al.* propose using neural networks for application performance prediction [14]. Meanwhile, Lee *et al.* formulate nonlinear regression models for performance and power prediction [21, 22]. Mosmodel [4] is a multi-input polynomial model used for virtual memory research that can predict the program execution time given the page table walking statistics. Wu *et al.* use performance counters as the input of ML models to predict GPU performance and power [46]. Nemirovsky *et al.* schedule threads based on ML-based performance models [25]. Some approaches are proposed to predict a processor’s performance/power based on those obtained on different types of processors [5, 6, 27] or with different ISAs [50, 49].

While these works build performance models on a per-program/input basis, SIMNET works at the instruction level. Therefore, these application-centric approaches require generating training data and retraining models when target applications change, and the overhead of doing so is significant. On the other hand, SIMNET can directly simulate any application, making it much more flexible.

Simulation with Statistical Sampling. Instead of simulating the entire program, statistical simulation selectively simulates representative sampling units and infers the overall performance from these sample simulation results statistically [10]. SMARTS [47, 45] periodically switches between detailed and functional simulation to obtain an accurate CPI estimation with minimal detailed simulation. One key challenge in statistical simulation is to keep track of the microarchitecture state between detailed simulation fractions, especially cache states. To simulate the cache behavior accurately in statistical simulation, Nikoleris *et al.* propose using Linux KVM to monitor the reuse distance of selected cache lines [26]. Similarly, Sandberg *et al.* leverage hardware virtualization to fast-forward between samples, so different samples can be simulated in parallel [36]. Compared with our ML-based simulator, these methods cannot extract detailed execution insights, such as the CPI curves in Figure 5. Furthermore, SIMNET and statisti-

cal simulation can be used together to further accelerate the detailed simulation portions.

SimPoint records the basic block execution frequencies of individual sampling units and those of the whole program to select representative ones with the aim that the selected samples capture the overall execution behaviors well [40, 32]. Similarly, PinPoints uses dynamic binary instrumentation to find representative samples for X86 programs [30], and BarrierPoint applies sampling to multi-threaded simulation [9]. These methods require pre-analyzing the simulated program with a certain input, while our ML-based simulator can be applied directly to any program and input combination because of its instruction-centric approach.

ML for Other Architecture Research. In addition to the aforementioned uses, ML has been widely applied to many other computer architecture aspects, including microarchitecture design and energy/power optimization. Penney and Chen provide a comprehensive survey about ML applications to the computer architecture domain [31].

Traditional Simulation Acceleration. ZSim is an X86 simulator that supports many-core system simulation [35]. It decouples the simulation of individual cores and resources shared across cores, as well as adopts a simplified core model. As a result, it achieves ~ 10 MIPS for single-thread workload simulation on an Intel Sandy Bridge 16-core processor. SST [16] distributes the simulation of different components across Message Passing Interface (MPI) ranks to achieve parallel simulation. Field programmable gate array (FPGA)-based emulators run significantly faster than software simulators but require a huge amount of effort to develop and validate register-transfer level models [18]. In comparison, our work accelerates simulation from a different angle to make the most of widely available ML accelerators, such as GPUs.

6. Conclusions

This work proposes a new computer architecture simulation paradigm using ML. To the best of our knowledge, this effort is the first to demonstrate ML’s applicability to full-fledged architecture simulation. This new methodology significantly improves simulation performance without sacrificing accuracy. In addition to discrete-event, analytical, or other statistical approaches to architectural simulation/modeling, we maintain this new class of simulators will become a useful, valuable addition to the architect’s “bag-of-tools.” We recognize several advantages of this new approach.

- 1) We demonstrate that ML-based simulators can predict overall performance accurately, and they also qualitatively capture architecture and application behaviors.
- 2) ML is intrinsically easier to parallelize than discrete-event simulation. Moreover, ML-based simulators capitalize on modern computing technology that is tailored for boosting ML performance.
- 3) ML-based simulators generalize well to a large spectrum of application workloads. In our approach, this stems from building them around an instruction-level latency predictor.

Hence, the focus is on learning instruction behaviors rather than high-level program behaviors that are much more difficult to capture. 4) The training data are easy and fast to obtain. Potential sources of training data are multiple, including simplified models of simulators, actual execution of code on existing systems, or historical performance data.

Future Directions. More research is required to support the simulation of multi/many-core and distributed systems. Specifically, modeling communication using ML-based simulation is a priority research direction to be tackled.

References

- [1] Dgx a100: Universal system for ai infrastructure. 2020.
- [2] Riken simulator for fujitsu a64fx. 2020.
- [3] Martín Abadi, Paul Barham, Jianmin Chen, Zhifeng Chen, Andy Davis, Jeffrey Dean, Matthieu Devin, Sanjay Ghemawat, Geoffrey Irving, Michael Isard, et al. Tensorflow: A system for large-scale machine learning. In *12th {USENIX} symposium on operating systems design and implementation ({OSDI} 16)*, pages 265–283, 2016.
- [4] Mohammad Agbarya, Idan Yaniv, Jayneel Gandhi, and Dan Tsafir. Predicting execution times with partial simulations in virtual memory research: why and how. In *IEEE/ACM International Symposium on Microarchitecture (MICRO)*, Global Online Event, October 2020. (to appear).
- [5] Newsha Ardalani, Clint Lestourgeon, Karthikeyan Sankaralingam, and Xiaojin Zhu. Cross-architecture performance prediction (xapp) using cpu code to predict gpu performance. In *Proceedings of the 48th International Symposium on Microarchitecture, MICRO-48*, page 725–737, New York, NY, USA, 2015. Association for Computing Machinery.
- [6] I. Baldini, S. J. Fink, and E. Altman. Predicting gpu performance from cpu runs using machine learning. In *2014 IEEE 26th International Symposium on Computer Architecture and High Performance Computing*, pages 254–261, 2014.
- [7] Nathan Binkert, Bradford Beckmann, Gabriel Black, Steven K. Reinhardt, Ali Saidi, Arkaprava Basu, Joel Hestness, Derek R. Hower, Tushar Krishna, Somayeh Sardashti, and et al. The gem5 simulator. *SIGARCH Comput. Archit. News*, 39(2):1–7, August 2011.
- [8] James Bucek, Klaus-Dieter Lange, and Jóakim v. Kistowski. Spec cpu2017: Next-generation compute benchmark. In *Companion of the 2018 ACM/SPEC International Conference on Performance Engineering*, pages 41–42, 2018.
- [9] T. E. Carlson, W. Heirman, K. Van Craeynest, and L. Eeckhout. Barrierpoint: Sampled simulation of multi-threaded applications. In *2014 IEEE International Symposium on Performance Analysis of Systems and Software (ISPASS)*, pages 2–12, 2014.
- [10] T. M. Conte, M. A. Hirsch, and K. N. Menezes. Reducing state loss for effective trace sampling of superscalar processors. In *Proceedings International Conference on Computer Design. VLSI in Computers and Processors*, pages 468–477, 1996.
- [11] A. Gutierrez, J. Pusdesris, R. G. Dreslinski, T. Mudge, C. Sudanthi, C. D. Emmons, M. Hayenga, and N. Paver. Sources of error in full-system simulation. In *2014 IEEE International Symposium on Performance Analysis of Systems and Software (ISPASS)*, pages 13–22, 2014.
- [12] Kaiming He, Xiangyu Zhang, Shaoqing Ren, and Jian Sun. Deep residual learning for image recognition. In *Proceedings of the IEEE conference on computer vision and pattern recognition*, pages 770–778, 2016.
- [13] Sepp Hochreiter and Jürgen Schmidhuber. Long short-term memory. *Neural computation*, 9(8):1735–1780, 1997.
- [14] Engin İpek, Sally A. McKee, Rich Caruana, Bronis R. de Supinski, and Martin Schulz. Efficiently exploring architectural design spaces via predictive modeling. In *Proceedings of the 12th International Conference on Architectural Support for Programming Languages and Operating Systems, ASPLOS XII*, page 195–206, New York, NY, USA, 2006. Association for Computing Machinery.
- [15] Aamer Jaleel, Robert S Cohn, Chi-Keung Luk, and Bruce Jacob. CMPSim: A pin-based on-the-fly multi-core cache simulator. In *Proceedings of the Fourth Annual Workshop on Modeling, Benchmarking and Simulation (MoBS), co-located with ISCA*, pages 28–36, 2008.
- [16] Curtis L Janssen, Helgi Adalsteinsson, Scott Cranford, Joseph P Kenny, Ali Pinar, David A Evensky, and Jackson Mayo. A simulator for large-scale parallel computer architectures. *International Journal of Distributed Systems and Technologies (IJ DST)*, 1(2):57–73, 2010.
- [17] Norman P. Jouppi, Cliff Young, Nishant Patil, David Patterson, Gaurav Agrawal, Raminder Bajwa, Sarah Bates, Suresh Bhatia, Nan Boden, Al Borchers, Rick Boyle, Pierre-luc Cantin, Clifford Chao, Chris Clark, Jeremy Coriell, Mike Daley, Matt Dau, Jeffrey Dean, Ben Gelb, Tara Vazir Ghaemmaghami, Rajendra Gottipati, William Gulland, Robert Hagmann, C. Richard Ho, Doug Hogberg, John Hu, Robert Hundt, Dan Hurt, Julian Ibarz, Aaron Jaffey, Alek Jaworski, Alexander Kaplan, Harshit Khaitan, Daniel Killebrew, Andy Koch, Naveen Kumar, Steve Lacy, James Laudon, James Law, Diemthu Le, Chris Leary, Zhuyuan Liu, Kyle Lucke, Alan Lundin, Gordon MacKean, Adriana Maggiore, Maire Mahony, Kieran Miller, Rahul Nagarajan, Ravi Narayanaswami, Ray Ni, Kathy Nix, Thomas Norrie, Mark Omernick, Narayana Penukonda, Andy Phelps, Jonathan Ross, Matt Ross, Amir Salek, Emad Samadiani, Chris Severn, Gregory Sizikov, Matthew Snelham, Jed Souter, Dan Steinberg, Andy Swing, Mercedes Tan, Gregory Thorson, Bo Tian, Horia Toma, Erick Tuttle, Vijay Vasudevan, Richard Walter, Walter Wang, Eric Wilcox, and Doe Hyun Yoon. In-datacenter performance analysis of a tensor processing unit. In *Proceedings of the 44th Annual International Symposium on Computer Architecture, ISCA '17*, page 1–12, New York, NY, USA, 2017. Association for Computing Machinery.
- [18] Sagar Karandikar, Howard Mao, Donggyu Kim, David Biancolin, Alon Amid, Dayeol Lee, Nathan Pemberton, Emmanuel Amaro, Colin Schmidt, Aditya Chopra, Qijing Huang, Kyle Kovacs, Borivoje Nikolic, Randy Katz, Jonathan Bachrach, and Krste Asanović. Firesim: Fpga-accelerated cycle-exact scale-out system simulation in the public cloud. In *Proceedings of the 45th Annual International Symposium on Computer Architecture, ISCA '18*, page 29–42. IEEE Press, 2018.
- [19] P. Diederik Kingma and Lei Jimmy Ba. Adam: A method for stochastic optimization. *international conference on learning representations*, 2015.
- [20] Alex Krizhevsky, Ilya Sutskever, and Geoffrey E Hinton. Imagenet classification with deep convolutional neural networks. *Advances in neural information processing systems*, 25:1097–1105, 2012.
- [21] B. C. Lee and D. M. Brooks. Illustrative design space studies with microarchitectural regression models. In *2007 IEEE 13th International Symposium on High Performance Computer Architecture*, pages 340–351, 2007.
- [22] Benjamin C. Lee, David M. Brooks, Bronis R. de Supinski, Martin Schulz, Karan Singh, and Sally A. McKee. Methods of inference and learning for performance modeling of parallel applications. In *Proceedings of the 12th ACM SIGPLAN Symposium on Principles and Practice of Parallel Programming, PPOPP '07*, page 249–258, New York, NY, USA, 2007. Association for Computing Machinery.
- [23] Scott M Lundberg and Su-In Lee. A unified approach to interpreting model predictions. In I. Guyon, U. V. Luxburg, S. Bengio, H. Wallach, R. Fergus, S. Vishwanathan, and R. Garnett, editors, *Advances in Neural Information Processing Systems 30*, pages 4765–4774. Curran Associates, Inc., 2017.
- [24] Charith Mendis, Alex Renda, Saman Amarasinghe, and Michael Carbin. Ithermal: Accurate, portable and fast basic block throughput estimation using deep neural networks. In *International Conference on Machine Learning*, pages 4505–4515. PMLR, 2019.
- [25] Daniel Nemirovsky, Tugberk Arkose, Nikola Markovic, Mario Nemirovsky, Osman Unsal, and Adrian Cristal. A machine learning approach for performance prediction and scheduling on heterogeneous cpus. In *2017 29th International Symposium on Computer Architecture and High Performance Computing (SBAC-PAD)*, pages 121–128, 2017.
- [26] Nikos Nikolieris, Lieven Eeckhout, Erik Hagersten, and Trevor E. Carlson. Directed statistical warming through time traveling. In *Proceedings of the 52nd Annual IEEE/ACM International Symposium on Microarchitecture, MICRO '52*, pages 1037–1049, New York, NY, USA, 2019. Association for Computing Machinery.
- [27] Kenneth O’neal, Philip Brisk, Ahmed Abousamra, Zack Waters, and Emily Shriver. Gpu performance estimation using software rasterization and machine learning. *ACM Trans. Embed. Comput. Syst.*, 16(5s), September 2017.
- [28] Adam Paszke, Sam Gross, Francisco Massa, Adam Lerer, James Bradbury, Gregory Chanan, Trevor Killeen, Zeming Lin, Natalia Gimelshein, Luca Antiga, Alban Desmaison, Andreas Kopf, Edward Yang, Zachary DeVito, Martin Raison, Alykhan Tejani, Sasank Chilamkurthy, Benoit Steiner, Lu Fang, Junjie Bai, and Soumith Chintala. Pytorch: An imperative style, high-performance deep learning library. In H. Wallach, H. Larochelle, A. Beygelzimer, F. d’Alché-Buc, E. Fox,

- and R. Garnett, editors, *Advances in Neural Information Processing Systems*, volume 32, pages 8026–8037. Curran Associates, Inc., 2019.
- [29] A. Patel, F. Afram, S. Chen, and K. Ghose. Marss: A full system simulator for multicore x86 cpus. In *2011 48th ACM/EDAC/IEEE Design Automation Conference (DAC)*, pages 1050–1055, 2011.
- [30] H. Patil, R. Cohn, M. Charney, R. Kapoor, A. Sun, and A. Karunanidhi. Pinpointing representative portions of large intel® itanium® programs with dynamic instrumentation. In *37th International Symposium on Microarchitecture (MICRO-37'04)*, pages 81–92, Dec 2004.
- [31] Drew D Penney and Lizhong Chen. A survey of machine learning applied to computer architecture design. *arXiv preprint arXiv:1909.12373*, 2019.
- [32] Erez Perelman, Greg Hamerly, Michael Van Biesbrouck, Timothy Sherwood, and Brad Calder. Using simpoint for accurate and efficient simulation. *SIGMETRICS Perform. Eval. Rev.*, 31(1):318–319, June 2003.
- [33] Alex Renda, Yishen Chen, Charith Mendis, and Michael Carbin. Diff-tune: Optimizing cpu simulator parameters with learned differentiable surrogates. In *IEEE/ACM International Symposium on Microarchitecture*, 2020.
- [34] David E Rumelhart, Geoffrey E Hinton, and Ronald J Williams. Learning representations by back-propagating errors. *nature*, 323(6088):533–536, 1986.
- [35] Daniel Sanchez and Christos Kozyrakis. Zsim: Fast and accurate microarchitectural simulation of thousand-core systems. *SIGARCH Comput. Archit. News*, 41(3):475–486, June 2013.
- [36] A. Sandberg, N. Nikolieris, T. E. Carlson, E. Hagersten, S. Kaxiras, and D. Black-Schaffer. Full speed ahead: Detailed architectural simulation at near-native speed. In *2015 IEEE International Symposium on Workload Characterization*, pages 183–192, 2015.
- [37] M. Sato, Y. Ishikawa, H. Tomita, Y. Kodama, T. Odajima, M. Tsuji, H. Yashiro, M. Aoki, N. Shida, I. Miyoshi, K. Hirai, A. Furuya, A. Asato, K. Morita, and T. Shimizu. Co-design for a64fx many-core processor and "fugaku". In *SC20: International Conference for High Performance Computing, Networking, Storage and Analysis*, pages 1–15, 2020.
- [38] André Seznec. TAGE-SC-L Branch Predictors Again. In *5th JILP Workshop on Computer Architecture Competitions (JWAC-5): Championship Branch Prediction (CBP-5)*, Seoul, South Korea, June 2016.
- [39] Lloyd S Shapley. A value for n-person games. *Contributions to the Theory of Games*, 2(28):307–317, 1953.
- [40] Timothy Sherwood, Erez Perelman, Greg Hamerly, and Brad Calder. Automatically characterizing large scale program behavior. In *Proceedings of the 10th International Conference on Architectural Support for Programming Languages and Operating Systems, ASPLOS X*, page 45–57, New York, NY, USA, 2002. Association for Computing Machinery.
- [41] Mingxing Tan, Bo Chen, Ruoming Pang, Vijay Vasudevan, Mark Sandler, Andrew Howard, and Quoc V. Le. Mnasnet: Platform-aware neural architecture search for mobile. In *Proceedings of the IEEE/CVF Conference on Computer Vision and Pattern Recognition (CVPR)*, June 2019.
- [42] Mingxing Tan and Quoc Le. EfficientNet: Rethinking model scaling for convolutional neural networks. In Kamalika Chaudhuri and Ruslan Salakhutdinov, editors, *Proceedings of the 36th International Conference on Machine Learning*, volume 97 of *Proceedings of Machine Learning Research*, pages 6105–6114. PMLR, 09–15 Jun 2019.
- [43] Han Vanholder. Efficient inference with tensorsrt, 2016.
- [44] Ashish Vaswani, Noam Shazeer, Niki Parmar, Jakob Uszkoreit, Llion Jones, Aidan N Gomez, Łukasz Kaiser, and Illia Polosukhin. Attention is all you need. In *Advances in neural information processing systems*, pages 5998–6008, 2017.
- [45] T. F. Wenisch, R. E. Wunderlich, M. Ferdman, A. Ailamaki, B. Falsafi, and J. C. Hoe. Simflex: Statistical sampling of computer system simulation. *IEEE Micro*, 26(4):18–31, 2006.
- [46] Gene Wu, Joseph L. Greathouse, Alexander Lyashevsky, Nuwan Jayasena, and Derek Chiou. Gpgpu performance and power estimation using machine learning. In *2015 IEEE 21st International Symposium on High Performance Computer Architecture (HPCA)*, pages 564–576, 2015.
- [47] Roland E. Wunderlich, Thomas F. Wenisch, Babak Falsafi, and James C. Hoe. Smarts: Accelerating microarchitecture simulation via rigorous statistical sampling. In *Proceedings of the 30th Annual International Symposium on Computer Architecture, ISCA '03*, page 84–97, New York, NY, USA, 2003. Association for Computing Machinery.
- [48] Toshio Yoshida. Fujitsu high performance cpu for the post-k computer. In *Hot Chips*, volume 30, 2018.
- [49] Xinnian Zheng, Lizy K. John, and Andreas Gerstlauer. Accurate phase-level cross-platform power and performance estimation. In *Proceedings of the 53rd Annual Design Automation Conference, DAC '16*, New York, NY, USA, 2016. Association for Computing Machinery.
- [50] Xinnian Zheng, Pradeep Ravikumar, Lizy K John, and Andreas Gerstlauer. Learning-based analytical cross-platform performance prediction. In *2015 International Conference on Embedded Computer Systems: Architectures, Modeling, and Simulation (SAMOS)*, pages 52–59. IEEE, 2015.